Stabilizing and characterizing unstable states in high-dimensional systems from time series

Valery Petrov,[1] Eugene Mihaliuk,[1] Stephen K. Scott,[2] and Kenneth Showalter[1,*]
[1]*Department of Chemistry, West Virginia University, Morgantown, West Virginia 26506-6045*
[2]*School of Chemistry, University of Leeds, Leeds LS2 9JT, United Kingdom*
(Received 13 December 1994)

An algorithm for stabilizing, characterizing, and tracking unstable steady states and periodic orbits in multidimensional dynamical systems is presented. The algorithm requires only one variable to be monitored and only one parameter to be perturbed for the stabilization of states with many unstable degrees of freedom and possibly an infinite number of stable degrees of freedom. The system is identified in terms of a linear recursive model with coefficients determined from successive readings of the variable subject to small random perturbations of the parameter. These coefficients determine the appropriate perturbations for control and also provide a direct route to the eigenvalues of the autonomous system. Spatially extended systems with an infinite number of degrees of freedom can be reduced to n effective dimensions that involve all the unstable manifolds and the weakly attracting stable manifolds. The remaining highly attracting manifolds are treated as one lumped eigenvector with an eigenvalue close to zero. The algorithm also allows the effective dimension of the state to be determined.

PACS number(s): 05.45.+b, 82.40.Py, 82.40.Bj

I. INTRODUCTION

Major strides have been made over the past few years in controlling chaos in low-dimensional systems [1]. Unstable periodic orbits have been stabilized in magnetoelastic strips [2], electronic circuits [3,4], laser systems [5,6], and chemical reactions [7–9], and recent reports of stabilizing periodic rhythms in heart tissue [10] and inducing periodic and chaotic behavior in hippocampal brain tissue [11] have stimulated widespread interest. It is clear that new developments in controlling dynamical systems offer opportunities for potentially important practical applications.

Several theoretical approaches have been advanced for stabilizing periodic orbits in chaotic systems. The feedback method proposed by Ott, Grebogi, and Yorke (OGY) [1,12] and the various modifications of this method have been the most popular. The OGY method is appealing because it is easily understood in terms of the system state in phase space. Stabilizing an unstable orbit simply involves perturbing the system such that the stable manifold of the orbit is targeted at each return. Thus, the positions of the system state and fixed point are known (in a suitable Poincaré section), and the effect of the perturbation is explicitly defined. Other control methods, including the continuous feedback algorithm of Pyragas [13,14], are described and compared to the OGY method by Alsing, Gavrielides, and Kovanis [15].

In systems that can be described by effectively one-dimensional (1D) maps, the OGY method can be reduced to an algorithm that directly targets the fixed point rather than the stable manifold [16,17]. The reduced algorithm is attractive for experimental applications because it requires minimal computational effort [3,5,7]. It can also be easily modified to permit tracking unstable steady and periodic states through bifurcation sequences [18,19]. Unstable periodic orbits [4,20] and steady states [21–23] have also been tracked with techniques that minimize fluctuations around the targeted fixed point.

It is known that the simple map-based approach may fail, even when a system is low dimensional and governed by a 1D map [17]. This arises when the fixed point is shifted away from the unstable manifold of the original attractor as the parameter is perturbed. In such cases, the perturbed system can no longer be described in terms of the shifted 1D map, which causes the method to fail. Rollins, Parmananda, and Sherard [24] have recently proposed a recursive algorithm that corrects for this effect. They added a linear recursive term to the map-based algorithm, following an earlier suggestion by Dressler and Nitsche [25] for modifying the OGY method when time-delay coordinates are used. This yields a one-variable, one-parameter method that allows stabilization in the otherwise pathological case when the fixed point is shifted away from the original unstable manifold [8].

Stabilizing and tracking states with more than one unstable direction remains an important challenge. Such states are common in spatially extended systems, and techniques beyond those developed for low-dimensional systems will be required for controlling spatiotemporal chaos. Simple techniques may be successful in certain spatiotemporal systems, such as when the behavior is highly spatially correlated [19]. Spatiotemporal chaos has also been controlled in a convectively unstable system, where the stabilized behavior is swept into the surrounding regions [26]. Proportional feedback has been used to stabilize periodic behavior in a coupled map lattice by multiple pinnings at locally stabilized sites, where the density of sites is increased until ordered behavior is exhibited [27]. Auerbach *et al.* [28] have proposed a

*Author to whom correspondence should be addressed.

 ©1995 The American Physical Society

generalization of the OGY approach, applicable to systems with one unstable and many stable degrees of freedom. Romerias *et al.* [29] have developed an approach for stabilizing states with multiple unstable directions and have applied this to a kicked double rotor model. It was necessary, however, to monitor all of the system variables for control.

In this paper, we present a general method for stabilizing and characterizing states with many unstable degrees of freedom and possibly an infinite number of stable degrees of freedom. This generalization provides an explicit connection between the OGY and related phase space approaches and the linear control routines of classical single-input single-output (SISO) systems [30]. The stabilization of high-dimensional unstable steady or periodic states requires only one system variable to be monitored and only one system parameter to be perturbed. The essential features of the approach are illustrated in Sec. II by considering a simple two-variable system, beginning with the case in which the system variables can be monitored directly and then generalizing this to a single experimental observable. A generalization of the approach to an n-dimensional system is described in Sec. III. The algorithm is applied in Sec. IV to stabilize and characterize an unstable four-cell flame front of the Kuramoto-Sivashinsky equation, which is found to have six unstable degrees of freedom. The method is also applied to stabilize and track a periodic orbit with two unstable directions. The advantages and limitations of the approach along with potential applications are described in Sec. V.

II. TWO-VARIABLE SYSTEM ILLUSTRATION

A geometric description of the general stabilization method can be developed by considering its application to a simple two-variable system. The system behavior around the unstable steady state is described by two linearized equations. Discrete dynamics is assumed, reflecting an experimental setting in which the system is sampled and perturbed at a fixed rate. Oscillatory behavior in the vicinity of an unstable periodic orbit can be reduced to linear discrete-time equations by using a suitable Poincaré section.

For illustration purposes, we imagine that ξ_1 and ξ_2, the coordinates along the system eigenvectors, are monitored at regular time intervals to give the set of data pairs $(\xi_{1,i},\xi_{2,i})$. If the ith point lies away from the fixed point $(\xi_{1,F},\xi_{2,F})$ and if the characteristic exponents describing the motion along the eigenvectors are λ_1 and λ_2, respectively, then the discrete-time equations of motion for the $i+1$ point are

$$\begin{aligned}\xi_{1,i+1}-\xi_{1,F}&=\lambda_1(\xi_{1,i}-\xi_{1,F})\ ,\\ \xi_{2,i+1}-\xi_{2,F}&=\lambda_2(\xi_{2,i}-\xi_{2,F})\ .\end{aligned}\tag{1}$$

For convenience, we assume that the fixed point lies at the origin: $(\xi_{1,F},\xi_{2,F})=(0,0)$. If, however, we also impose a small perturbation on some parameter p, the position of the fixed point is shifted along some line in phase space by an amount proportional to the perturbation. Denoting this perturbation as p_{i+1}, the evolution equations now become

$$\begin{aligned}\xi_{1,i+1}&=\lambda_1\xi_{1,i}+(1-\lambda_1)\alpha_1 p_{i+1}\ ,\\ \xi_{2,i+1}&=\lambda_2\xi_{2,i}+(1-\lambda_2)\alpha_2 p_{i+1}\ ,\end{aligned}\tag{2}$$

where the coefficients α_1 and α_2 are the projections of the shift vector $\partial\xi_F/\partial p$ determining the change in the fixed point position along the corresponding eigenvectors with change in the parameter p.

If a second perturbation p_{i+2} is made at the next step, the second iteration will be given by

$$\begin{aligned}\xi_{1,i+2}&=\lambda_1^2\xi_{1,i}+(1-\lambda_1)\alpha_1(\lambda_1 p_{i+1}+p_{i+2})\ ,\\ \xi_{2,i+2}&=\lambda_2^2\xi_{2,i}+(1-\lambda_2)\alpha_2(\lambda_2 p_{i+1}+p_{i+2})\ .\end{aligned}\tag{3}$$

Note that the eigenvalues are assumed to be independent of the parameter perturbation, at least to leading order. From Eq. (3) it follows that $\xi_{1,i+2}$ and $\xi_{2,i+2}$ can be set equal to zero by an appropriate choice of the perturbations p_{i+1} and p_{i+2}, which are found as a solution of the linear system provided $\lambda_1\neq\lambda_2$ and $\alpha_i\neq 0$. The requirement of the system eigenvalues to be nonequal and the parameter perturbation to displace the system along all of the unstable manifolds are the main conditions for achieving stabilization of multivariable systems using a single parameter.

Figure 1 shows an application with $\lambda_1=1.5$ and $\lambda_2=3$, where the system has evolved away from the unstable fixed point at the origin to the point marked **0**. In the first perturbation, the fixed point is moved along the shift vector $\partial\xi_F/\partial p$ to $\xi_F^1=(\xi_{1,F},\xi_{2,F})^1$. The system state evolves relative to the shifted fixed point according to the multipliers to the point marked **1**. In the second perturbation, the fixed point is moved again along the shift vec-

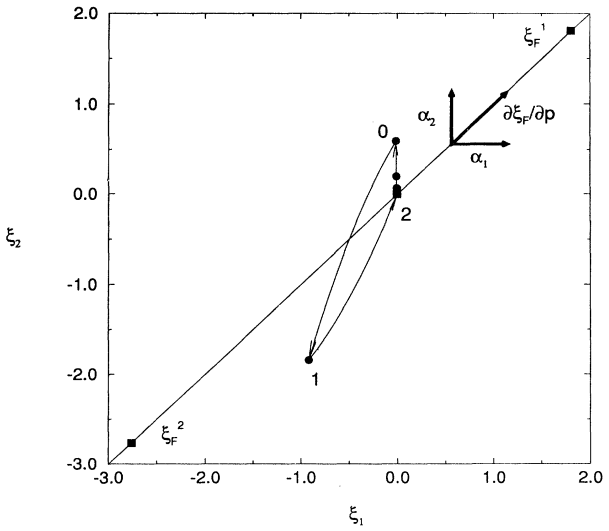

FIG. 1. Geometrical description of control method. Application to a two-variable system with a fixed point characterized by $\lambda_1=1.5$ and $\lambda_2=3$. Two successive perturbations cause the system to evolve from point **0** to point **2**, corresponding to the fixed point of the unperturbed system.

tor to $\xi_F^2=(\xi_{1,F},\xi_{2,F})^2$. The system now evolves relative to this fixed point position to the point marked 2, which corresponds to the targeted fixed point of the unperturbed system.

This example provides a graphical description of the targeting procedure; however, it differs from the operational procedure in that the sequence of n controlling perturbations must be determined in advance. In real-time applications of the algorithm, the value of the controlling perturbation is updated at each step. For the two-variable example, the $i+1$ perturbation is

$$p_{i+1}=k_1\xi_{1,i}+k_2\xi_{2,i} , \tag{4}$$

where the coefficients k_1 and k_2 are chosen to ensure that the fixed point is targeted on the second iteration. There are several possibilities for finding the appropriate k_1 and k_2 when the system coordinates or all independent system variables are known. The approach originally suggested by OGY targets the stable manifold of a state with one unstable direction [12]. If the fixed point has two unstable manifolds, it can still be targeted using Eq. (4) with two successive perturbations [29]. In the absence of noise, control equations (3) and (4) each produce the same sequence of two perturbations for targeting the fixed point.

In experimental settings, we commonly do not have access to the actual system variables, nor can we monitor n independent observable variables. Time-delay embedding techniques can be used to reconstruct the system state around a periodic orbit [12] provided that a correction for the shift of the Poincaré section is carried out [25,28,29]. Here we present a general approach for reconstructing the system state from the readings of one observable variable in the presence of perturbations. The approach is applicable to system dynamics on a Poincaré section or around a steady state.

In general, we monitor some observable x that is a linear combination of the system variables. For our two-variable illustration, we have

$$x_i=t_1\xi_{1,i}+t_2\xi_{2,i} . \tag{5}$$

The choice of variable x is largely unrestricted; however, the expected unstable behavior must be observable by monitoring x.

We will show that the system state vectors ξ, scaled by projection coefficients t_i, can be reconstructed from successive readings of x and p. We rewrite Eqs. (2) for $i-1$ and then sum the first multiplied by $\lambda_2 t_1$ with the second multiplied by $\lambda_1 t_2$, and with Eq. (5) for $i-1$ obtain

$$\lambda_1\lambda_2 x_{i-1}+[\lambda_2(1-\lambda_1)\alpha_1 t_1+\lambda_1(1-\lambda_2)\alpha_2 t_2]p_i =\lambda_2 t_1\xi_{1,i}+\lambda_1 t_2\xi_{2,i} . \tag{6}$$

The system state $(t_1\xi_{i,1},t_2\xi_{i,2})$ can therefore be found as a solution of Eqs. (5) and (6) from the x_i, x_{i-1}, and p_i, provided that $\lambda_1\neq\lambda_2$. The control equation (4) can then be written as

$$p_{i+1}=q_2 x_i+q_1 x_{i-1}+r_1 p_i , \tag{7}$$

where coefficients q_1, q_2, and r_1 can be expressed through the system parameters. It follows from Eq. (6) that the term involving x_{i-1} disappears from the control equation in the case when one of the manifolds is strongly attracting (for which $\lambda_2\approx 0$). This corresponds to the recursive feedback algorithm of Rollins, Parmananda, and Sherard [24] for the control of highly dissipative systems. It also follows from Eq. (6) that when the perturbation does not significantly shift the fixed point off the unstable manifold ($\lambda_2\approx 0$ and $\alpha_2\approx 0$) the simple map-based algorithm [16,17] is recovered.

We show in Sec. III that n successive readings of the observable x and $n-1$ values of the previous perturbations are required to control an n-dimensional system. We also show how the coefficients q_1, q_2, and r_1 of the control equation can be found, along with other system unknowns, from the time series of the experimental observable.

System identification and control

The control algorithm requires that the dynamical system be continuously *interrogated* by imposing random perturbations on a suitable parameter p at regular sampling intervals. The time series obtained by recording some observable x then consists of a set of data pairs:

$$(x_1,p_1),(x_2,p_2),(x_3,p_3),\ldots,(x_i,p_i) . \tag{8}$$

For a system with two independent variables, we need to record at least seven data pairs (i.e., $3n+1$) to allow identification of the system. Control can then begin with the parameter perturbation p_8.

The time series can be fitted to a recursive SISO model [30] of the form

$$x_{i+1}=a_2 x_i+a_1 x_{i-1}+a_0+b_2 p_{i+1}+b_1 p_i . \tag{9}$$

This form is also known as an autoregressive with auxiliary input (ARX) equation [31]. The number of fitting coefficients a and b and their relation to the system parameters is discussed in Sec. III. For the two-dimensional system, $n=2$ and there are five unknowns: a_0–a_2, b_1, and b_2. Applying this approach to obtain the data pairs in (8) produces a set of five equations, which we can write explicitly as

$$\begin{aligned} x_3&=a_2 x_2+a_1 x_1+a_0+b_2 p_3+b_1 p_2 ,\\ &\vdots\\ x_7&=a_2 x_6+a_1 x_5+a_0+b_2 p_7+b_1 p_6 , \end{aligned} \tag{10}$$

where the coefficient a_0 is related to the fixed point x_F by

$$a_0=(1-a_2-a_1)x_F . \tag{11}$$

We note that $a_0=0$ if $x_F=0$, which we assume in the following treatment. (Alternatively, the optimal values of the coefficients could be determined more precisely from a larger data set using singular value decomposition, but here we proceed from this minimum basis set.)

The eigenvalues λ_1 and λ_2 governing the "autonomous" system, i.e., the system in the absence of perturbations, can be determined from the a_i coefficients.

Motion along the ith eigenvector occurs with $x_n \propto \lambda_i^n$, and substituting the corresponding terms into (9) yields the characteristic equation for the system eigenvalues:

$$-\lambda^2+a_2\lambda+a_1=0 \ . \tag{12}$$

The eigenvalues of the "closed-loop" system under control can be obtained by deriving the recursive model in a form that does not depend on the perturbations. We obtain the perturbation-independent equation by combining Eqs. (7) and (9) to express p_{i+1}:

$$p_{i+1}=\frac{r_1x_{i+1}+(b_1q_2-r_1a_2)x_i+(b_1q_1-r_1a_1)x_{i-1}}{r_1b_2+b_1} \ . \tag{13}$$

Equation (13) for p_i and p_{i+1} can be substituted into Eq. (9), allowing x_{i+1} to be expressed as a linear combination of x_i, x_{i-1}, and x_{i-2}:

$$x_{i+1}=l_3x_i+l_2x_{i-1}+l_1x_{i-2} \ , \tag{14}$$

where

$$l_3=r_1+a_2+b_2q_2, \quad l_2=a_1-r_1a_2+b_1q_2+b_2q_1 \ , \quad l_1=b_1q_1-a_1r_1 \ . \tag{15}$$

The controlled system is described by Eq. (14) and is characterized by a total of three eigenvalues, λ_1,λ_2, and λ_3, which can be found as roots of the polynomial

$$-\lambda^3+l_3\lambda^2+l_2\lambda+l_1=0 \ . \tag{16}$$

We achieve stabilization using the pole placement technique, i.e., by requiring these eigenvalues to adopt the target values λ_1^*,λ_2^*, and λ_3^*. The roots of Eq. (16) will have the appropriate values of λ_i^* when

$$l_1=\lambda_1^*\lambda_2^*\lambda_3^*, \quad l_2=-(\lambda_1^*\lambda_2^*+\lambda_2^*\lambda_3^*+\lambda_3^*\lambda_1^*) \ , \quad l_3=\lambda_1^*+\lambda_2^*+\lambda_3^* \ . \tag{17}$$

There is some freedom in selecting the target values. In general, we require $|\lambda_i^*|<1$ so the system converges toward the fixed point: the smaller the magnitude of the target eigenvalues, the faster the convergence will be. When all of the eigenvalues of the system under control are chosen to be zero (so-called "deadbeat" control) the system should converge to the steady state after n iterations. This, however, may involve the imposition of larger perturbations at the early stages of control. One approach is to leave the stable eigenvalues unchanged. This control results in targeting the corresponding stable manifolds rather than the fixed point and reduces the magnitude of the control perturbations. It is important to note that setting the eigenvalues close to unity is dangerous, since even small errors in the system identification can then make the system unstable. Also, if the system is high dimensional, errors in the system parameters that are inevitably carried over from the identification stage may become large. Selecting the optimal control law in the presence of system parameter errors is the subject of the H_∞ control approach [32].

The various coefficients a_0-a_2, b_1,b_2, and l_1-l_3 are now used to calculate the required perturbation to be imposed at the next time step:

$$p_8=q_2x_7+q_1x_6+q_0+r_1p_7 \ . \tag{18}$$

Here q_1, q_2, and r_1 are given by the solutions of Eqs. (15) and (17) and q_0 is assumed to be zero (which is equivalent to $x_F=0$). This perturbation is applied at the seventh sampling time. The process is then repeated, with the appropriate perturbation p_9 being calculated from x_8, x_7, and p_8.

III. GENERALIZATION TO AN n-VARIABLE SYSTEM

The control algorithm can be generalized to apply to a system of dimensionality n. The coefficients a_0-a_n and b_1-b_n are determined by fitting the recursive SISO model to at least $3n+1$ data pairs collected from the interrogated system (i.e., the system subjected to random perturbations at each sampling time) and the target values selected for the eigenvalues of the controlled system.

If a sequence of n perturbations p_2 to p_{n+1} is applied to an n-dimensional system, the following equations can be written for n consecutive iterations of the state vector ξ (i.e., the coordinates along the system eigenvectors):

$$\begin{aligned}
&\xi_1=\xi_1 \ , \\
&\xi_2=\hat{\lambda}\xi_1+(\hat{I}-\hat{\lambda})p_2\boldsymbol{\alpha} \ , \\
&\xi_3=\hat{\lambda}^2\xi_1+(\hat{I}-\hat{\lambda})(p_2\hat{\lambda}+p_3)\boldsymbol{\alpha} \ , \\
&\vdots \\
&\xi_{n+1}=\hat{\lambda}^n\xi_1+(\hat{I}-\hat{\lambda})(p_2\hat{\lambda}^{n-1}+\cdots+p_n\hat{\lambda}+p_{n+1})\boldsymbol{\alpha} \ ,
\end{aligned} \tag{19}$$

where

$$\hat{\lambda}=\begin{bmatrix}\lambda_1 & 0 & 0\\ 0 & \ddots & 0\\ 0 & 0 & \lambda_n\end{bmatrix}, \quad \hat{I}=\begin{bmatrix}1 & 0 & 0\\ 0 & \ddots & 0\\ 0 & 0 & 1\end{bmatrix}, \quad \boldsymbol{\alpha}=\frac{\partial\xi_F}{\partial p} \ . \tag{20}$$

In the general case, the observable variable x is a linear combination of ξ_i,

$$x=\mathbf{t}\cdot\xi \ . \tag{21}$$

We can therefore rewrite the last equation of (19) as

$$x_{n+1}=(\boldsymbol{\lambda}^n\hat{t}\xi_1)+(\mathbf{p}_{n+1}L(\hat{I}-\hat{\lambda})\hat{t}\boldsymbol{\alpha}) \ , \tag{22}$$

where

$$L=\begin{bmatrix}\lambda_1^{n-1} & \cdots & \lambda_n^{n-1}\\ \vdots & & \vdots\\ \lambda_1 & \cdots & \lambda_n\\ 1 & \cdots & 1\end{bmatrix}, \quad \boldsymbol{\lambda}^n=\begin{bmatrix}\lambda_1^n\\ \vdots\\ \lambda_n^n\end{bmatrix} \ ,$$

$$\hat{t}=\begin{bmatrix}t_1 & 0 & 0\\ 0 & \ddots & 0\\ 0 & 0 & t_n\end{bmatrix}, \quad \mathbf{p}_{n+1}=\begin{bmatrix}p_2\\ \vdots\\ p_{n+1}\end{bmatrix} \ . \tag{23}$$

We can further rearrange Eq. (22) to express x_{n+1} as a function of $\mathbf{x}_n=(x_1,\ldots,x_n)$ and $\mathbf{p}_{n+1}=(p_2,\ldots,p_{n+1})$:

$$x_{n+1}=(\mathbf{a}\cdot\mathbf{x}_n)+[\alpha\hat{t}(\underline{I}-\hat{\lambda})L^T A\,\mathbf{p}_{n+1}]\ , \tag{24}$$

where

$$\mathbf{a}=\begin{bmatrix}1 & \lambda_1 & \cdots & \lambda_1^{n-1}\\ \vdots & \vdots & & \vdots\\ 1 & \lambda_n & \cdots & \lambda_n^{n-1}\end{bmatrix}^{-1}\lambda^n\ ,$$
$$A=\begin{bmatrix}1 & 0 & \cdots & 0\\ -a_n & 1 & & \vdots\\ \vdots & & \ddots & 0\\ -a_2 & \cdots & -a_n & 1\end{bmatrix}\ . \tag{25}$$

Equation (24) can be rewritten as

$$x_{i+1}=a_n x_i+a_{n-1}x_{i-1}+\cdots+a_1 x_{i-n+1}+a_0+b_n p_i+\cdots+b_1 p_{i-n+1}\ . \tag{26}$$

Equations (24)–(26) provide the connection between the coefficients a_i, b_i, and the phase space description of the system, as used in the OGY control algorithm. Specifically, the eigenvalues of the system are the roots of the polynomial

$$-\lambda^n+a_n\lambda^{n-1}+\cdots+a_2\lambda+a_1=0\ , \tag{27}$$

and the b_i coefficients are linear combinations of the projections of the shift vector. Equation (24) is related to the Laplace transformation from the state space realization to the transfer function widely used in classical control theory [30].

The $2n+1$ unknown coefficients of Eq. (26) can be calculated from the time series of a single observable variable. If n is the dimensionality of the system, then $3n+1$ successive readings of the variable and $3n+1$ corresponding perturbations are required for the solution. Since n previous perturbations and observations are required to predict the future of the system according to Eq. (26), the control law should involve the same number of variables.

The control perturbation for the $i+1$ step is calculated from the equation

$$p_{i+1}=q_n x_i+q_{n-1}x_{i-1}+\cdots+q_1 x_{i-n+1}+q_0+r_{n-1}p_i+\cdots+r_1 p_{i-n+1}\ , \tag{28}$$

using the pole placement technique for recursive models [30]. The coefficients q_1-q_n and r_1-r_{n-1} are the solution of the linear system

$$\begin{bmatrix}a_n & -1 & 0 & \cdots & 0 & b_n & 0 & 0 & \cdots & 0\\ a_{n-1} & a_n & -1 & \cdots & 0 & b_{n-1} & b_n & 0 & \cdots & 0\\ \cdot & \cdot & \cdot & \cdots & -1 & \cdot & \cdot & \cdot & \cdot & 0\\ a_1 & a_2 & \cdot & \cdots & a_n & b_1 & b_2 & \cdot & \cdots & b_n\\ 0 & a_1 & \cdot & \cdots & a_{n-1} & 0 & b_1 & \cdot & \cdots & b_{n-1}\\ 0 & 0 & \cdot & \cdots & \cdot & 0 & 0 & \cdot & \cdots & \cdot\\ 0 & 0 & 0 & \cdot\ 0 & a_1 & 0 & 0 & 0 & \cdot\cdot & b_1\end{bmatrix}\begin{bmatrix}1\\ -r_{n-1}\\ \cdot\\ -r_1\\ q_n\\ \cdot\\ \cdot\\ q_1\end{bmatrix}=\begin{bmatrix}l_{2n-1}\\ \cdot\\ \cdot\\ \cdot\\ \cdot\\ \cdot\\ l_1\end{bmatrix}\ , \tag{29}$$

where the l_i are the $2n-1$ coefficients that correspond to the target eigenvalues of the controlled system:

$$-\lambda^{*2n-1}+l_{2n-1}\lambda^{*2n-2}+\cdots+l_2\lambda^*+l_1=0\ . \tag{30}$$

We note that the overall dimensionality of the controlled system is increased by $(n-1)$.

In general, the dimensionality of the system will not be known in advance. Nor can the effective number of degrees of freedom always be deduced from the evolution of the autonomous system in the linear region of the unstable fixed point. The parameter perturbations used for control may shift the system onto stable manifolds not evident in the unperturbed case and reveal additional dimensions. On the other hand, the effective dimensionality can be determined by interrogating the system with the method outlined above. For spatiotemporal systems, most of the infinite number of modes will decay rapidly compared to the sampling period. We follow the suggestion by Auerbach *et al.* [28] of lumping all the highly attracting manifolds together as one. The effective dimensionality is therefore equal to the number of unstable and slowly attracting stable manifolds plus one. The method of determining n will be illustrated with reference to a particular example in the next section.

IV. STABILIZING HIGH-DIMENSIONAL STATES OF THE KURAMOTO-SIVASHINSKY EQUATION

The Kuramoto-Sivashinsky (KS) equation is one of the simplest nonlinear partial differential equations for modeling spatiotemporal chaos. It has been found to mimic the dynamical behavior of many different physical systems, but is most often used to model the spatiotemporal evolution of 2D flame fronts [33]. The governing equation for the contour of the front has the form

$$\frac{\partial\psi}{\partial t}-\left[\frac{\partial\psi}{\partial z}\right]^2+\frac{\partial^2\psi}{\partial z^2}+\frac{\partial^4\psi}{\partial z^4}=0\ . \tag{31}$$

We use the KS equation as an example of a multidimensional system that can be stabilized with the control algorithm. With a reaction zone width of $L=35.0$, a symmetrical four-cell solution is found to be unstable and

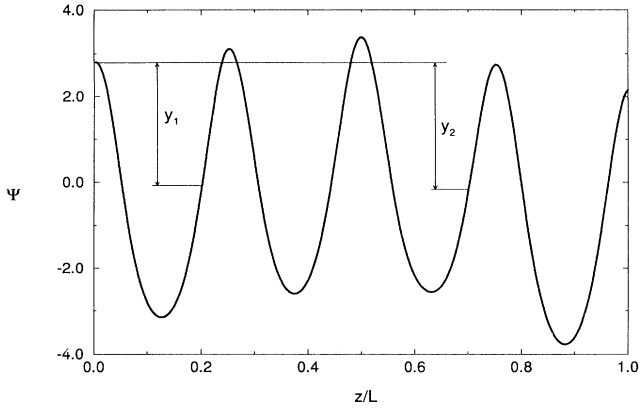

FIG. 2. Four-cell solution of the KS equation for the system width $L=35.0$. The symmetrical solution is unstable at this value of L, and this profile shows a snapshot in the early evolution away from the symmetrical state. The observables $y_1=\Psi(0)-\Psi(0.2)$ and $y_2=\Psi(0)-\Psi(0.7)$ are used to monitor the spatiotemporal evolution of the profile.

the system diverges away from this state to exhibit spatiotemporal chaos. Figure 2 shows the front as it moves away from the symmetrical state and the two quantities, y_1 and y_2, that serve as the "experimental" observables to monitor the spatiotemporal evolution of the profile. A two-dimensional projection of the phase portrait constructed from these observables is shown in Fig. 3, where the system is evolving away from the unstable state. Although the evolution of the system is followed very close to the unstable state, it is clear that the behavior is high dimensional. Generally, the time series of only one observable variable provides enough information for control. Figure 4 shows the corresponding time series generated from the observable y_1, which is used as the monitored variable in the control algorithm. The points in

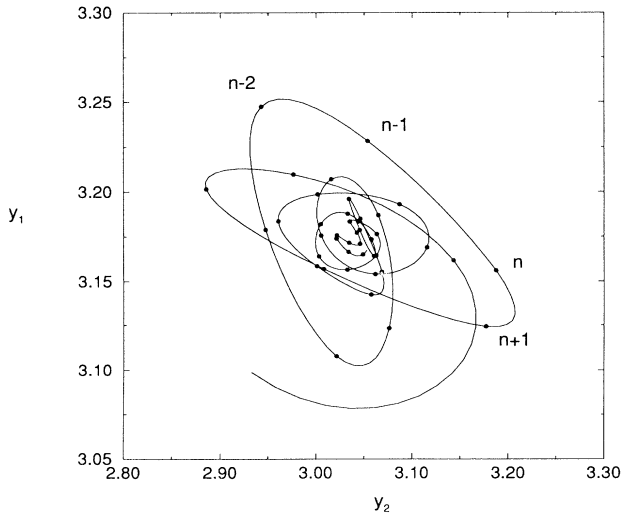

FIG. 3. Phase portrait showing evolution of system away from symmetrical four-cell solution. Two-dimensional projection is constructed from the observables y_1 and y_2.

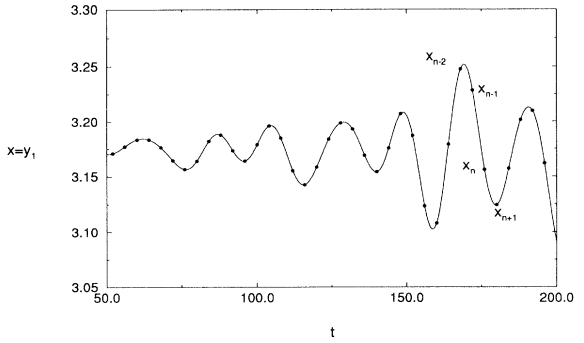

FIG. 4. Time series showing observable y_1 used in identification and control as the system evolves away from the symmetrical four-cell solution.

Figs. 3 and 4 show the sampling times of the monitored variable.

A. Determination of dimensionality

The evolution of the four-cell front away from the unstable symmetric solution—where a random perturbation is applied to a selected parameter at each sampling interval—is shown in the *identification* part of Fig. 5. The parameter chosen for perturbation is the gradient $\partial\psi/\partial z$ at $z=0$. The unperturbed boundary condition, corresponding to the autonomous system in Figs. 3 and 4, is $\partial\psi/\partial z=0$ at this point. In general we utilize "mirror" boundary conditions, where the first and third derivatives in Eq. (31) are required to be zero at the boundaries.

The data pairs (x_i,p_i) from the perturbed system (up to $t=250.0$ in Fig. 5) are used to determine the dimension and the corresponding eigenvalues of the autonomous system. Error estimates for different choices of n are obtained by summing the error between the measurements and the optimized n-dimensional fit to Eq. (26) over the entire data set. Figure 6 shows the variation of this error

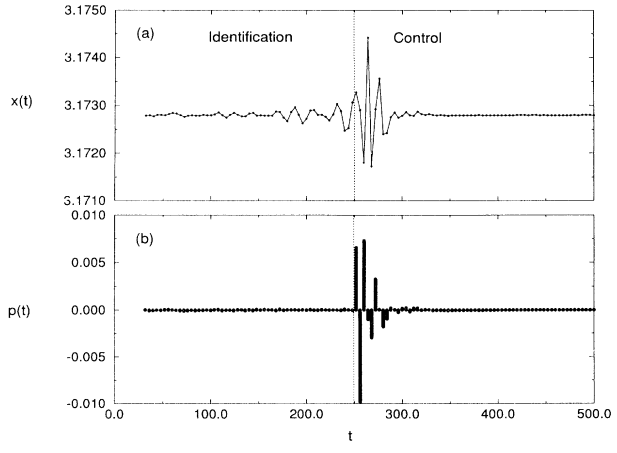

FIG. 5. Identification and control of the unstable symmetrical four-cell solution of the Kuramoto-Sivashinsky equation. (a) Value of observable x_i during identification and control phases, and (b) value of the controlling parameter p_{i+1}.

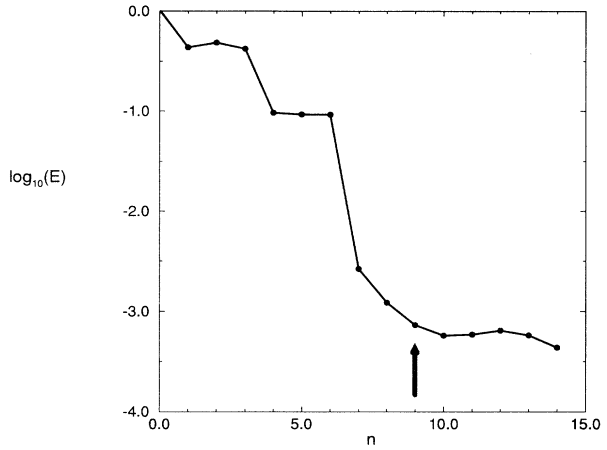

FIG. 6. Dependence of the fitting error of Eq. (26) on n, showing the plateau from $n=9$. An effective dimensionality of $n=9$ is used for stabilization of the symmetrical four-cell front shown in Fig. 2. Error E is calculated with respect to the standard deviation of the predicted amplitude error relative to the average amplitude of oscillation as shown in the *identification* stage of Fig. 5(a).

as a function of n. For $n \geq 9$, there is no significant reduction in the fitting error on increasing the effective dimension, so we choose $n=9$ for this system. It should be noted that the small error for convergence (typically 10^{-3} to 10^{-4}) suggests that it may be difficult to determine dimension from experimental data with this method due to the possibility of noise at higher magnitudes than the convergence criterion. The eigenvalues of the unstable four-cell solution are calculated as the roots of the equation

$$-\lambda^9+a_9\lambda^8+\cdots+a_2\lambda+a_1=0\ , \tag{32}$$

which are shown in Fig. 7. There are six unstable eigenvalues (modulus >1) and three stable eigenvalues, the latter corresponding to modes excited by the parameter perturbations. The eigenvalue of smallest magnitude represents the lumping of an infinite number of stable modes that decay quickly compared to the sampling interval.

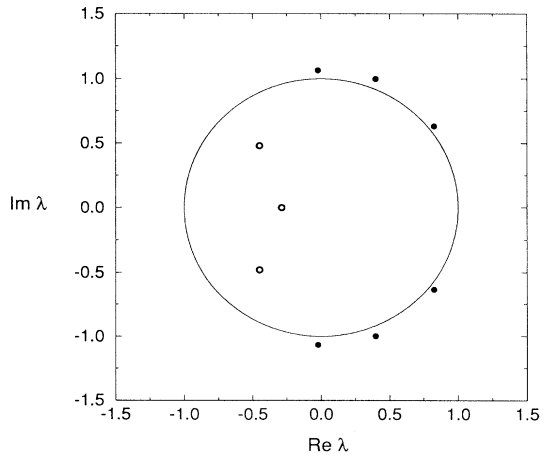

FIG. 7. Eigenvalues of the unstable four-cell solution calculated as roots of Eq. (32). Solid dots represent the unstable eigenvalues of the autonomous system. Open circles show the stable eigenvalues obtained by interrogating the system with random perturbations.

B. Stabilization of steady four-cell front

Once n and the coefficients a_i and b_i are determined, the algorithm is implemented in the control stage from $t=250.0$. All the eigenvalues of the closed-loop system were chosen to be zero by setting $l_i=0$ in Eq. (29). As indicated in Fig. 5, the state is effectively stabilized after the first cycle of nine perturbations. The control algorithm is applied continuously, with the values of the coefficients revised after each sampling and then used to calculate the next perturbation. In the present example, the magnitude of the control perturbations becomes very small after two cycles, or on the 19th iteration of the algorithm. We note that stabilization was also achieved with assumed system dimensionalities of $n=10$ and 11. The higher-order control laws are less desirable in experimental settings, however, due to their higher sensitivity to errors.

C. Stabilization of periodic two-cell front

The Kuramoto-Sivashinsky equation exhibits fronts with different numbers of cells on increasing the reaction zone width L. Each of these fronts loses its temporal stability through a bifurcation sequence that leads to chaotic behavior before the next front with more cells is established. We now examine the spatiotemporal behavior of a two-cell front in order to apply the control algorithm to a periodic orbit with more than one unstable direction. Specifically, we will stabilize and track a period-1 limit cycle through a secondary Hopf bifurcation, where the orbit is characterized by two unstable directions. The oscillatory front is monitored by recording the position of the minimum in the front profile. The minimum in the temporal oscillations is then used as the system observable. This choice eliminates the need to construct the $n-1$ dimensional Poincaré section in time-delay coordinates and is therefore convenient for monitoring high-dimensional periodic states of unknown dimensionality. Possible shifts of the attractor [25] do not cause difficulties because such effects are automatically incorporated into Eq. (24) from the identification procedure. The bifurcation diagram is shown in Fig. 8, where the minimum of oscillation is plotted as a function of the reaction zone width. (Further examples of spatiotemporal behavior in the two-cell KS front along with a detailed description of the monitoring technique can be found in Ref. [19].)

The two-cell solution exhibits period-1 oscillations at a reaction zone width of $L=20.7$, where we begin tracking. As the width is decreased, the period-1 orbit becomes unstable through a secondary Hopf bifurcation at $L=20.57$ with the appearance of quasiperiodic behavior. At $L=20.4$, the imaginary part of the eigenvalues responsible for the quasiperiodic behavior become zero and two

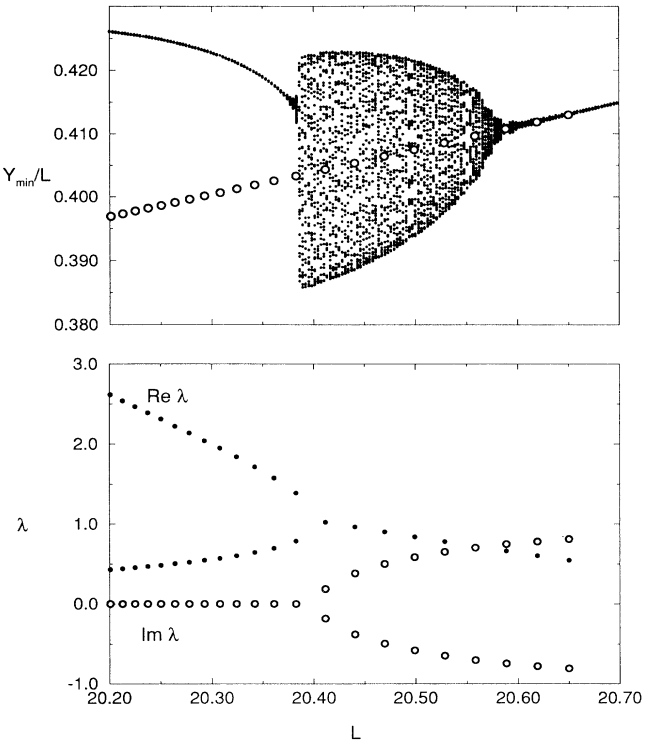

FIG. 8. Bifurcation diagram showing quasiperiodic behavior of the two-cell front of the KS equation. (a) Solid points show minimum of oscillations of front profile minimum. Open circles show the symmetrical oscillatory state tracked from right to left through the secondary Hopf bifurcation and quasiperiodic oscillations to the region where the unsymmetrical period-1 oscillation is stable. (b) The real (Re) and imaginary (Im) parts of the eigenvalues as a function of L shown by solid and open circles, respectively.

new period-1 solutions appear. As L is decreased further, the quasiperiodic behavior enters the basin of attraction of one of the stable period-1 solutions and nonsymmetric periodic oscillations are exhibited.

The symmetric period-1 solution was stabilized and tracked through the range of L shown in Fig. 8 (a) using the control algorithm with $n=2$. The controlling perturbation of the boundary condition was found to introduce a negligible displacement along the stable manifolds; therefore, it was necessary to explicitly consider only two unstable degrees of freedom for control. The algorithm was applied according to Eq. (28), with small random perturbations added to the control perturbations to interrogate the system. This technique allows the coefficients to be updated every time the bifurcation parameter is changed by repeating the identification procedure. The eigenvalues of the periodic state were calculated from the roots of Eq. (12) and are shown in Fig. 8 (b).

V. CONCLUSIONS

A general method for the control of unstable steady or periodic states of dynamical systems has been presented. The algorithm requires only a single observable quantity and acts through perturbations imposed on a single system parameter. For an n-dimensional system, n previous observations and $n-1$ previous perturbations are required for control. The states that are stabilized under this control correspond directly to the states of the autonomous system. The algorithm also provides a full characterization of the autonomous state in terms of its effective dimensionality and eigenvalues. The approach can be readily applied to experimental systems without any knowledge of the underlying mechanism or governing equations.

The effective reduction of high-dimensional dynamics to a single variable makes the method especially useful for stabilizing spatiotemporal systems by small perturbations localized in space. Local perturbations were sufficient for stabilizing stationary and periodic behavior in the Kuramoto-Sivashinsky equation. We note, however, that this approach may be less successful in spatiotemporal systems with a lower degree of spatial correlation. Local application of the algorithm in such systems will likely result in stabilization only within a correlation radius.

Selection of a particular unstable behavior is also possible using the control algorithm. Setting one of the closed-loop eigenvalues to be the same as the eigenvalue of a chosen unstable manifold will result in a control law that stabilizes all but the selected unstable manifold. This approach requires only very small perturbations and can be used to manipulate the dynamics of a high-dimensional system by observing only a single variable. The method may provide a more precise implementation of "anticontrol" recently demonstrated in experiments with hippocampal brain tissue [11].

When coupled with tracking techniques, the algorithm provides a model-independent, path-following method for the bifurcation analysis of experimental systems. The availability of the eigenvalues means that the character of bifurcations in experimental systems can be determined directly, rather than by inference from observations of qualitative changes in the time series. The algorithm can also be used to extend the parameter range of desired responses, such as stable burning in flame systems or steady output in high-dimensional lasers. It should also be noted that even though the method has been illustrated using a discrete-time approach, it can be reformulated in a continuous-time framework. Such a modification might allow the stabilization of very fast processes by using a control law that is precalculated and then implemented with an analog circuit.

ACKNOWLEDGMENTS

We thank the National Science Foundation (Grant No. CHE-9222616) and the Office of Naval Research (Grant No. N00014-95-1-0247) for supporting this research. Acknowledgment is made to the donors of The Petroleum Research Fund, administered by the American Chemical Society, for partial support of this research.

[1] T. Shinbrot, C. Grebogi, E. Ott, and J. A. Yorke, Nature **363**, 411 (1993).
[2] W. L. Ditto, S. N. Rauseo, and M. L. Spano, Phys. Rev. Lett. **65**, 3211 (1990).
[3] E. R. Hunt, Phys. Rev. Lett. **67**, 1953 (1991).
[4] T. Carroll, I. Triandaf, I. B. Schwartz, and L. Pecora, Phys. Rev. A **46**, 6189 (1992).
[5] R. Roy, T. W. Murphy, T. D. Maier, Z. Gills, and E. R. Hunt, Phys. Rev. Lett. **68**, 1259 (1992).
[6] S. Bielawski, D. Derozeir, and P. Glorieux, Phys. Rev. A **47**, R2492 (1993).
[7] V. Petrov, V. Gáspár, J. Masere, and K. Showalter, Nature **361**, 240 (1993).
[8] P. Parmananda, P. Sherard, R. W. Rollins, and H. D. Dewald, Phys. Rev. E **47**, R3003 (1993).
[9] F. W. Schneider, R. Blittersdorf, A. Förster, T. Hauck, D. Lebender, and J. Müller, J. Phys. Chem. **97**, 12 244 (1993).
[10] A. Garfinkel, M. L. Spano, W. L. Ditto, and J. N. Weiss, Science **257**, 1230 (1992).
[11] S. J. Schiff, K. Jerger, D. H. Duong, T. Chang, M. L. Spano, and W. L. Ditto, Nature **370**, 615 (1994).
[12] E. Ott, C. Grebogi, and J. A. Yorke, Phys. Rev. Lett. **64**, 1196 (1990).
[13] K. Pyragas, Phys. Lett. A **170**, 421 (1992).
[14] K. Pyragas and A. Tamasevicius, Phys. Lett. A **180**, 99 (1993).
[15] P. M. Alsing, A. Gavrielides, and V. Kovanis, Phys. Rev. E **50**, 1968 (1994).
[16] B. Peng, V. Petrov, and K. Showalter, J. Phys. Chem. **95**, 4957 (1991).
[17] V. Petrov, B. Peng, and K. Showalter, J. Chem. Phys. **96**, 7506 (1992).
[18] V. Petrov, M. F. Crowley, and K. Showalter, Phys. Rev. Lett. **72**, 2955 (1994).
[19] V. Petrov, M. F. Crowley, and K. Showalter, J. Chem. Phys. **101**, 6606 (1994).
[20] S. Bielawski, D. Derozeir, and P. Glorieux, Phys. Rev. E **49**, R971 (1994).
[21] Z. Gills, C. Iwata, R. Roy, I. B. Schwartz, and I. Triandaf, Phys. Rev. Lett. **69**, 3169 (1992).
[22] A. Hjelmfelt and J. Ross, J. Phys. Chem. **94**, 1176 (1994).
[23] S. Bielawski, M. Bouazaoui, D. Derozeir, and P. Glorieux, Phys. Rev. A **47**, 3276 (1993).
[24] R. W. Rollins, P. Parmananda, and P. Sherard, Phys. Rev. E **47**, R780 (1993).
[25] U. Dressler and G. Nitsche, Phys. Rev. Lett. **68**, 1 (1992).
[26] D. Auerbach, Phys. Rev. Lett. **72**, 1184 (1994).
[27] G. Hu and Z. Qu, Phys. Rev. Lett. **72**, 68 (1994).
[28] D. Auerbach, C. Grebogi, E. Ott, and J. A. Yorke, Phys. Rev. Lett. **69**, 3479 (1992).
[29] F. J. Romerias, C. Grebogi, E. Ott, and W. P. Dayawansa, Physica D **58**, 165 (1992).
[30] G. C. Goodwin and K. S. Sin, *Adaptive Filtering, Prediction, and Control* (Prentice-Hall, Englewood Cliffs, NJ, 1984).
[31] L. Ljung, *System Identification—Theory for the User* (Prentice-Hall, Englewood Cliffs, NJ, 1987).
[32] J. C. Dole, K. Glover, P. Khargonekar, and B. Francis, IEEE Trans. Automat. Contr. **34**, 1831 (1989).
[33] G. I. Sivashinsky, Annu. Rev. Fluid Mech. **15**, 179 (1983).